13TH CANADIAN MASONRY SYMPOSIUM
HALIFAX, CANADA
JUNE 4TH – JUNE 7TH 2017

THREE-DIMENSIONAL FINITE ELEMENT MODEL FOR MASONRY INFILLED RC FRAMES SUBJECTED TO OUT-OF-PLANE LOADING

Nasiri, Ehsan[1] and Liu, Yi[2]

ABSTRACT

The literature review revealed that masonry infills bounded by either steel or RC frames may develop out-of-plane strength much higher than their flexural strength due to arching action. However, the available technical information on this subject is limited and the current Canadian masonry standard S304-14 does not contain design equations to calculate the out-of-plane strength of masonry infills. Several existing analytical methods were largely based on the empirical test results conducted mainly on steel frames and they fail to capture the effects of different geometric and mechanical behaviour of masonry infills, and boundary conditions between the masonry infill and the frame. This paper presents the development of a finite element model for simulating out-of-plane behaviour of concrete masonry infilled RC frames. Developed in ABAQUS software, this FE model adopted a three dimensional simplified micro modeling technique considering detailed geometry and nonlinear characteristics of concrete, steel and masonry units. The model was validated against experimental results of two specimens including one regular infilled frame and one with opening in the infill. The comparison between the FE and experimental results in terms of ultimate strength, load vs. displacement response, and cracking and failure modes is described in the paper. The FE model developed in this study was found to be capable of simulating the out-of-plane behaviour and strength of masonry infilled RC frames and capturing the cracking pattern and failure modes with reasonable accuracy.

KEYWORDS: *masonry infill, out-of-plane, RC frame, arching action, finite element*

INTRODUCTION

The out-of-plane behaviour and strength of masonry walls bounded by reinforced concrete (RC) or steel frames is an important aspect of structural design for buildings subjected to out-of-plane forces such as wind and earthquake. Early experimental work [1-3] has shown that the masonry

[1] PhD Candidate, Department of Civil and Resource Engineering, Dalhousie University, 5248 Morris St., Halifax, NS, Canada, Ehsan.Nasiri@dal.ca
[2] Professor, Department of Civil and Resource Engineering, Dalhousie University, 5248 Morris St., Halifax, NS, Canada, yi.liu@dal.ca

infills had much greater capacity than that predicted by flexural analysis and this capacity increase was enabled by a mechanism referred to as “arching action”. When a wall is butted up against the frame acting as rigid supports, in-plane compressive forces are induced in the wall as it bends under out-of-plane forces, and this compressive forces can delay cracking and restrain subsequent arching of the wall, which ultimately leads to capacity increase. The arching action was confirmed in later experimental studies [1, 3-6] where an increase in the out-of-plane capacity, in some cases, 2 to 3 times higher than its flexural capacity has been reported. Even when gaps exist between the infill and the frame member, the arching may still develop only to a lesser degree [7]. The more recent research [8-11] showed that the arching action was dependent on the masonry compressive strength, infill dimensions, and boundary conditions between the infill and the frame. Development of arching action can enhance the stability of infills even after the ultimate capacity was achieved. However, parameters in previous studies were limited and although arching mechanism was well accepted, development of rational design equations to incorporate the effect of all influential parameters for practical design remains a challenge. For practice, the Canadian masonry design standard CSA S304-14 suggests that the first principle mechanics be relied on for analysis of the out-of-plane strength of infill walls. The American masonry design standard MSJC 2013 provides a strength equation for masonry infills based on experimental results mainly obtained by three research groups ([6, 9, 12]). Due to its semi-empirical nature, its efficacy for infilled frames different from those tested in terms of material and geometric properties has not been thoroughly examined. Numerical modeling encoded in computer programs has been increasingly used in simulating behaviour of masonry infilled frames. Many two-dimensional (2D) models developed using commercial software have shown success in simulation of in-plane behaviour of infilled frames. However, in the case of out-of-plane behaviour, the 2D models are not adequate to capture aspects of infilled frame behaviour such as non-typical geometric properties, stress concentration, local reinforcement effects which are critical for out-of-plane loading consideration. The three dimensional (3D) FE modeling is preferred in this case. The advancement of computer technology in recent years has made 3D models computationally efficient for its application in this field as evidenced by several studies [13-16]. However, since 3D modeling in the field of masonry infilled frames is still in its relatively new development stage, there is commonly a lack of information provided on the input material parameters in the existing 3D model studies, which makes it difficult for others to reproduce the model and associated results.

This study was then motivated to develop a 3D finite element model to study the out-of-plane behaviour of masonry infilled RC frames. The model was validated against results of masonry infilled RC frames tested in parallel with the finite element modelling. The model development and its behaviour parameters as well as the validation against the test results are detailed in this paper. It is shown that the model is capable of simulating out-of-plane behaviour and capturing cracking and failure modes of the infilled RC frame.

FINITE ELEMENT MODELING

In this study, the simplified micro-modelling approach [17] was adopted where the mortar joints are not physically modeled, rather, they are replaced with zero-thickness interface elements. The software ABAQUS was used in the modeling. The concrete masonry units (CMU) as well as RC frame members were modeled using solid elements. The CMU dimensions were increased by the half thickness of the mortar joint in both horizontal and vertical directions so that the discrete CMUs were connected and interact with each other through zero-thickness interface elements. The simplified micro-model has shown to provide desired accuracy [17, 18] and is considered as a more computing efficient modeling technique than a detailed micro-modelling approach where mortar joints are modelled. The geometry and the meshing of the model is shown in Figure 1.

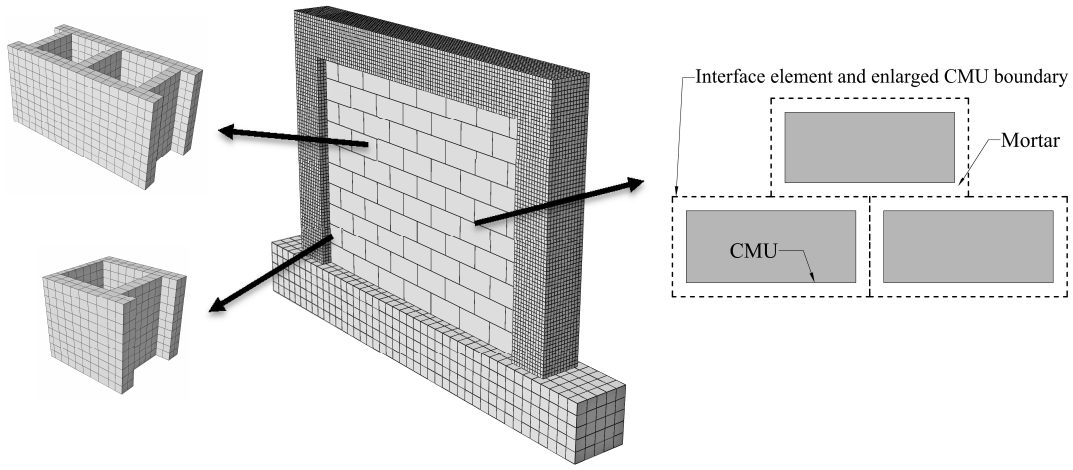

Figure 1: Three dimensional geometric model used in FE analysis

Behaviour model of masonry units and concrete

The Concrete Damaged Plasticity (CDP) model for quasi-brittle materials in ABAQUS [19] was used to simulate the behaviour of concrete and CMUs in this study. The CDP model is a continuum, plasticity-based, damage model. Both isotropic damaged elasticity and tensile and compressive plasticity are considered in this model and failure mechanisms are defined in terms of tensile cracking and compressive crushing.

The compressive behaviour of concrete and CMUs were defined by incorporating the experimentally obtained mechanical properties into the stress-strain constitutive model proposed by Sima et al. [20] and shown in Figure 2.

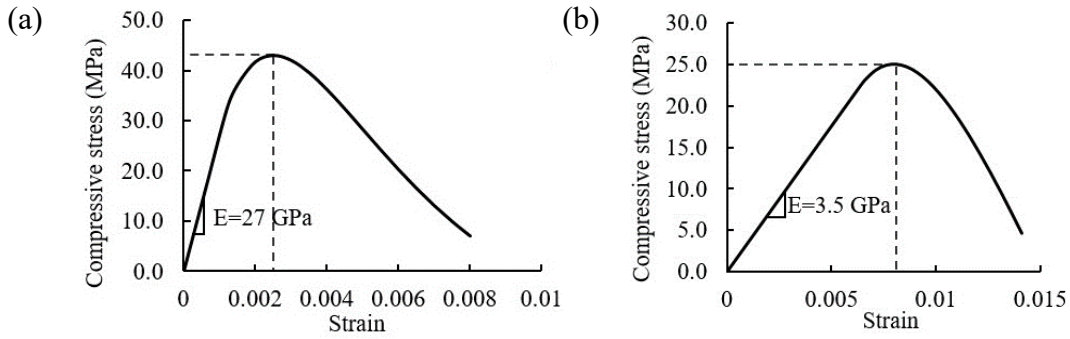

Figure 2: Compression stress-strain curve for: (a) Concrete; and (b) CMUs

For tensile behaviour, the Shima and Okamura [21] method was used to determine the stress-strain curve of concrete incorporating the tension stiffening effect of the reinforcement. In the case of CMUs, the tensile behaviour is more dependent on localized single crack which initiates a sharp stress drop. The tensile behaviour model for CMUs was defined by a linear elastic behaviour in the pre-cracking phase and a stress-crack displacement curve in the post-cracking phase as suggested by Fib: Model Code [22]. These curves are shown in Figure 3.

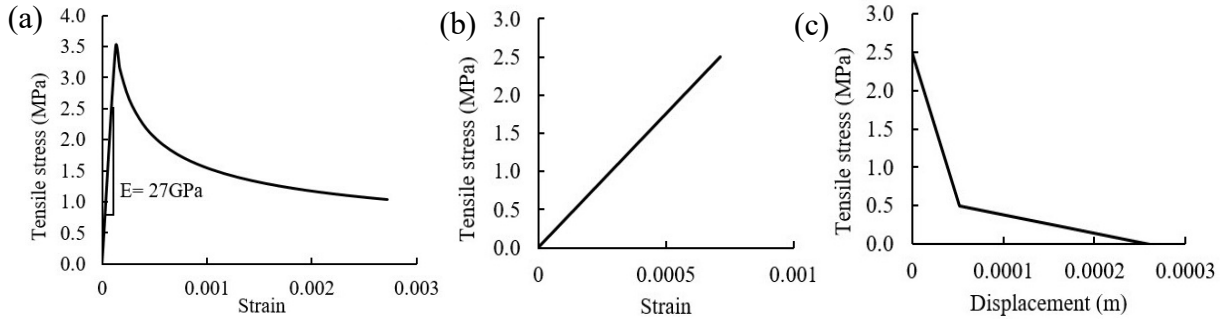

Figure 3: Tensile behaviour of concrete and CMU material: (a) stress-strain curve for concrete; (b) stress-strain curve for CMU; and (c) stress-displacement curve for CMU

Behaviour model of interface elements

To account for plastic behaviour and possible failure modes of the mortar joints, interface elements between CMUs adopted the surface-based cohesive behaviour in ABAQUS in combination with shear and tensile failure criteria. The surface-based cohesive behaviour provides a simplified micro approach to model the mortar using the traction-separation constitutive model. The shear and normal fracture and their corresponding energy releases were also implemented to allow for degradation and removal of the interaction after failure, at which point, interaction between the CMUs is controlled by Coulomb friction behaviour.

The traction-separation law includes three stages: linear elastic traction-separation, damage initiation criteria and damage evolution laws. In the elastic state, the behaviour is controlled by an elastic response for both normal and transverse deformations. The traction stress vector t consists of three components, t_n, t_s and t_t, which represent the tensile and two shear tractions.

The corresponding separations are denoted by δ_n, δ_s and δ_t. The elastic behaviour for this case in matrix form is expressed as:

$$t = \begin{Bmatrix} t_n \\ t_s \\ t_t \end{Bmatrix} = \begin{bmatrix} K_{nn} & 0 & 0 \\ 0 & K_{ss} & 0 \\ 0 & 0 & K_{tt} \end{bmatrix} \begin{Bmatrix} \delta_n \\ \delta_s \\ \delta_t \end{Bmatrix} = K\delta \quad (1)$$

Once failure is detected as tensile and shear stress reaching corresponding strengths, two damage models (normal and shear stress damage) control the degradation and elimination of the interaction using the fracture energy approach [17, 23]. In this approach, the areas under the traction-separation curves for tensile and shear after the peak stresses were set to be equal to the Mode I and Mode II fracture energy of the mortar material ([17, 23]). Upon the full degradation of the interface elements they were deleted from the model to allow for the Coulomb frictional contact between the masonry units. At this stage, contacting surfaces can carry shear stresses up to a certain magnitude before sliding, which is known as sticking. The critical shear stress at which sliding of the surfaces starts, is defined as $\tau_{crit} = \mu N$ where, N is the contact pressure and μ is the coefficient of friction. This behaviour model was also used for contact at the infill-to-frame member interface.

The behaviour of mortar joints is schematically illustrated in Figure 4.

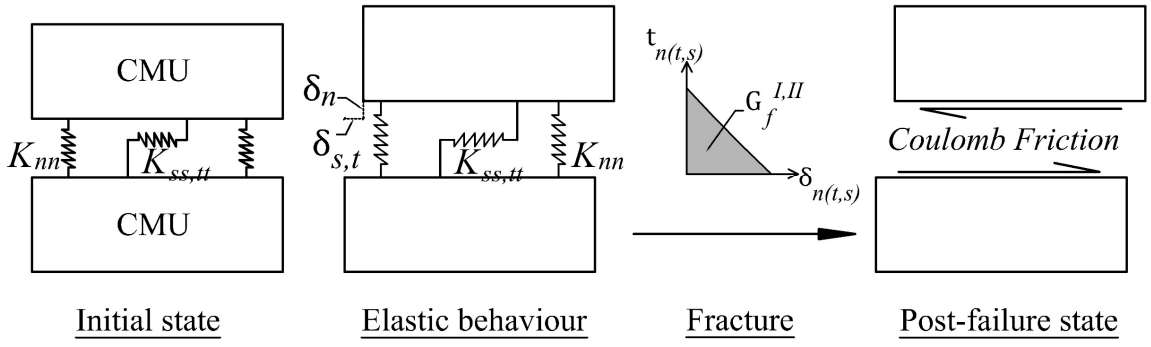

Figure 4: Behaviour of mortar joints

Table 1 summarizes values of input parameters used in the interface element modeling. The available literature was mainly relied upon for obtaining a reasonable range of values and the final value used was selected through an extensive calibration process against the experimental results obtained in this study.

EXPERIMENTAL PROGRAM

The experimental program involved testing of masonry infilled RC frames of various parameters subjected to a monotonically increased out-of-plane pressure. In this paper, the results obtained thus far, including a regular infilled frame (IFNG) as control specimen and an infilled frame with 16% (opening/infill area) window opening (IFW16) were used for validation of the model.

Table 1: Summary of interface parameters

Symbol	Description	Value	Unit	Source/Reference
E	Elastic modulus	2600	MPa	Experiment
ν	Poisson's ratio	0.16	-	Experiment
t_n^0	Tensile strength of mortar	0.2	MPa	[24-26]
$t_{s,t}^0$	Shear strength of mortar	1.0	MPa	[24-26]
G_f^{II}	Shear fracture energy	400	N/m	[25, 27]
G_f^I	Tension fracture energy	40	N/m	[25, 27]
μ	Coulomb friction coefficient	0.7	-	[18, 25, 27]

The dimensions and reinforcement details for the specimens are shown in Figure 5. The masonry infill was constructed using the custom-made, half-scale standard 200 mm concrete masonry units laid in the running bond. Type S mortar was used in construction with an average mortar joint thickness of 7 mm. The RC frame was designed according to CSA A23.3 2014 [28] and the reinforcement detailing including size, spacing, arrangement of longitudinal bars and stirrups complied with requirements to provide ductility and avoid brittle shear failure.

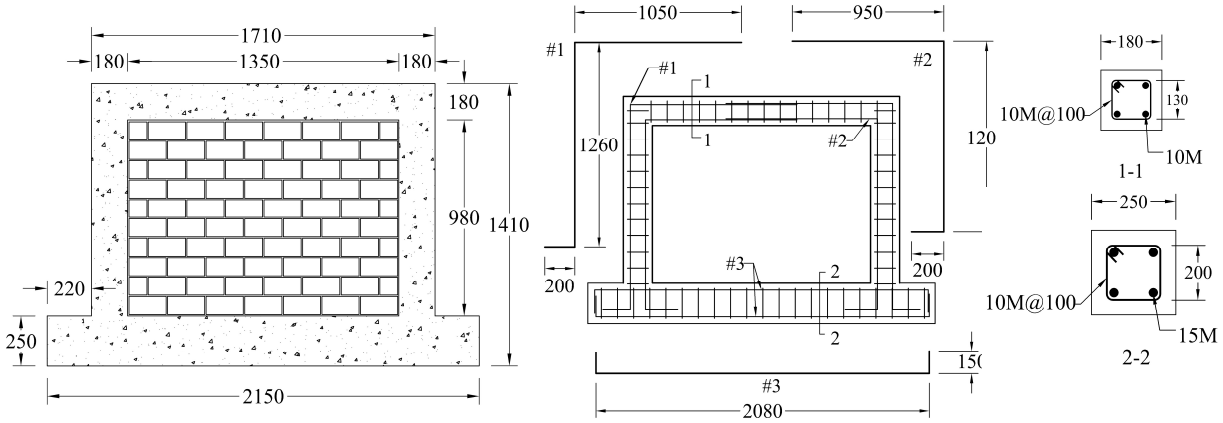

Figure 5: Dimension of infilled frame specimens and reinforcement details in the RC frame

The experimental set-up is illustrated in Figure 6. The specimens were clamped to the strong floor using steel W-sections on either end of the frame beam stem to prevent potential lateral or transverse movement. The out-of-plane loading was applied using an airbag through a self-equilibrating system as shown. The airbag was housed in a reaction box made of plywood boards stiffened with steel sections. The reaction box was connected to the RC frame using high strength threaded rods. An air compressor was used to inflate the airbag and the real-time

pressure was measured using a pressure transducer. Four linear variable differential transformers (LVDTs) were mounted at different locations on the back of the infill wall to measure the out-of-plane displacements. The air pressure was applied gradually at a rate of 1 kPa per minute until the failure of the specimen. The load and LVDT readings were monitored and recorded with an interval of 0.2 seconds throughout the test using an electronic data acquisition system. For each test, the cracking load, ultimate load, cracking pattern and failure mode were noted as necessary.

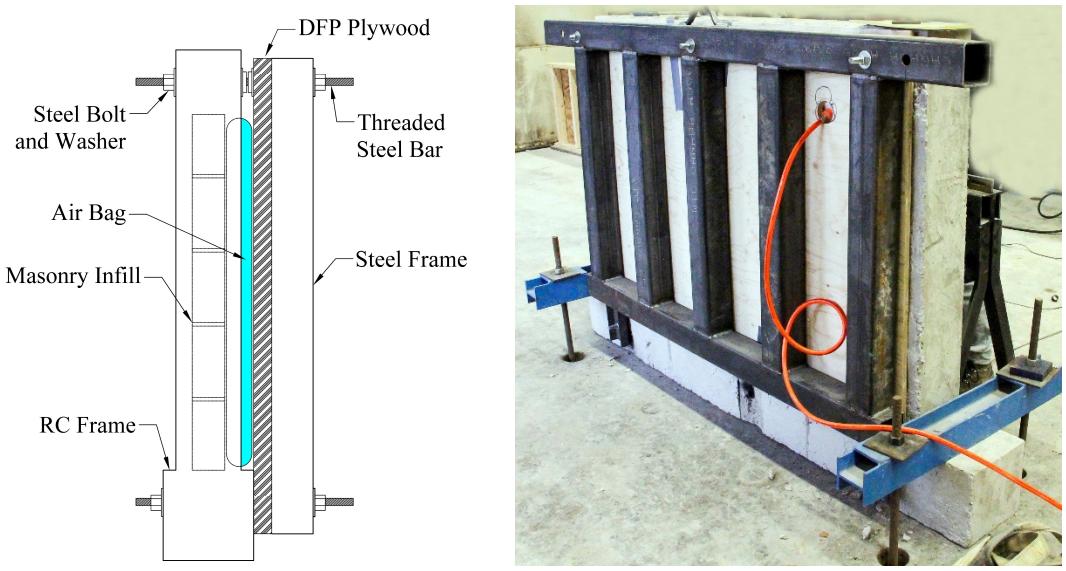

Figure 6: Test set-up for out-of-plane loading of the specimens

Mechanical properties of CMUs, mortar, and masonry prisms for the infill and those of concrete and reinforcement for the frame were obtained experimentally in accordance with ASTM specifications. A summary of the material properties is presented in Table 2.

Table 2: Summary of material properties for test specimens

	Elastic modulus E (MPa)	Compressive strength (MPa)	Tensile strength (MPa)	Yield strength (MPa)	Ultimate (yield) strain
Concrete	27800	43.8	3.5	-	0.0025
CMUs	3500	25.0	2.5	-	0.008
Mortar	2600	21.3	1.7	-	-
Prisms	2980	17.1	-	-	-
Reinforcement	220000	-	665	446	0.085 (0.003)

MODEL VALIDATION

The model was validated through important response parameters including stiffness and strength, load vs. displacement curves, and cracking and failure modes. The experimental-to-FE capacity ratio, $\frac{q_{u,\mathrm{EXP}}}{q_{u,\mathrm{FE}}}$, is determined to be 1.04 and 1.01 for IFNG and IFW16, respectively. This suggests

that the model is capable of accurately predicting the ultimate strength. The out-of-plane pressure versus displacement curves for IFNG and IFW16 obtained from the experiments and FE models are compared in Figure 7.

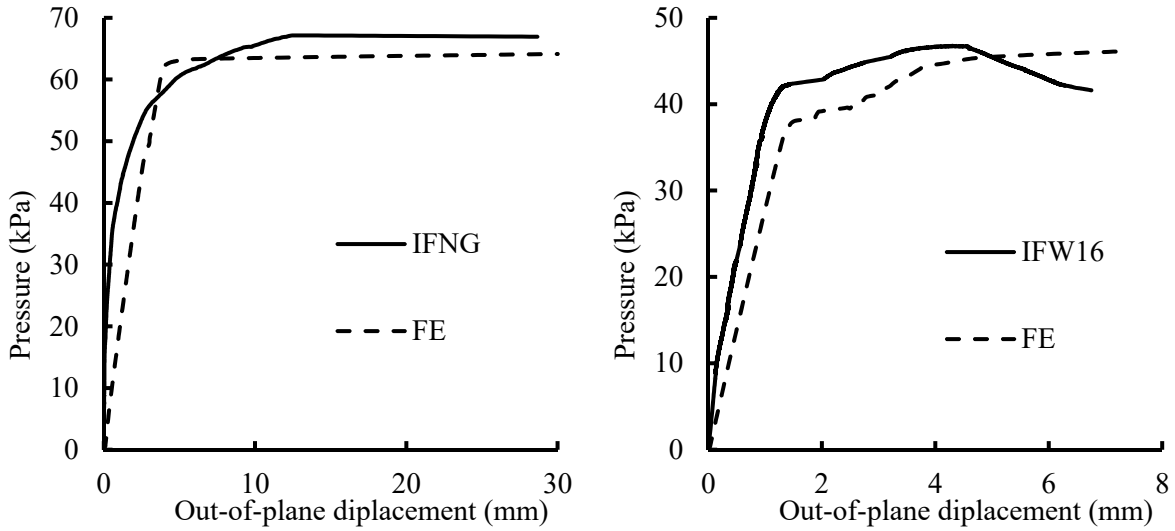

Figure 7: Comparison of out-of-plane pressure vs. displacement curves obtained from tests and FE analysis

The figure shows that the FE model, in general, can simulate the out-of-plane response of the infilled RC frames reasonably well. For specimen IFNG, both experimental and FE results showed that a horizontal crack first formed around the mid-height of the infill at early stage of loading (<10 kPa). This crack did not result in significant loss of stiffness and strength in the infill. As the pressure loading increased, the arching of the wall became more noticeable and the horizontal crack extended through the CMU blocks as well as the mortar joints towards the corners of the infill. However, there was still no significant drop of stiffness and strength, indicating that the arching action was the mechanism by which the infill was resisting the load. At about 70% of the ultimate load, the forces applied to the RC frame members by arched sections of the infill caused the in-plane bending of the frame beam, resulting in flexural cracks on the top of the frame beam. At the ultimate, failure was sudden and volatile characterized by the out-of-plane collapse of the infill. For specimen IFW16, a similar observation was made with the difference being that the initial cracks formed around the corners of the opening and extended towards the corners of the infill. As a result of the arching action, a more or less linear elastic response through the large portion of loading history would be expected. This is in line with FE curves and the experimental curve of IFW16. The nonlinearity shown in the experimental curve for IFNG was attributed to some early crushing observed at the mortar joints at the infill-to-frame boundary.

Figure 8 shows the deformed geometry, cracking pattern, and compressive crushing obtained from the experiments and FE model for IFW16. While Figure 8(a) shows the tensile cracking contour on the loading surface of the infill, Figure 8(b) shows the compressive crushing contour

in the mid-plane of the infill, enabled by 3D modelling for the stress distribution through blocks. The red contours shown in the FE results represent the regions where stresses were well beyond the cracking stress or compressive strength whereas the green contours represent the regions that just began to crack or crush. It can be seen that the FE model accurately simulated the cracking formed and developed in the infill and RC frame. The compressive stress contour shown in Figure 8(b) seems to suggest that collapse was initiated through shear failure of infill webs, which was in line with experimental observation.

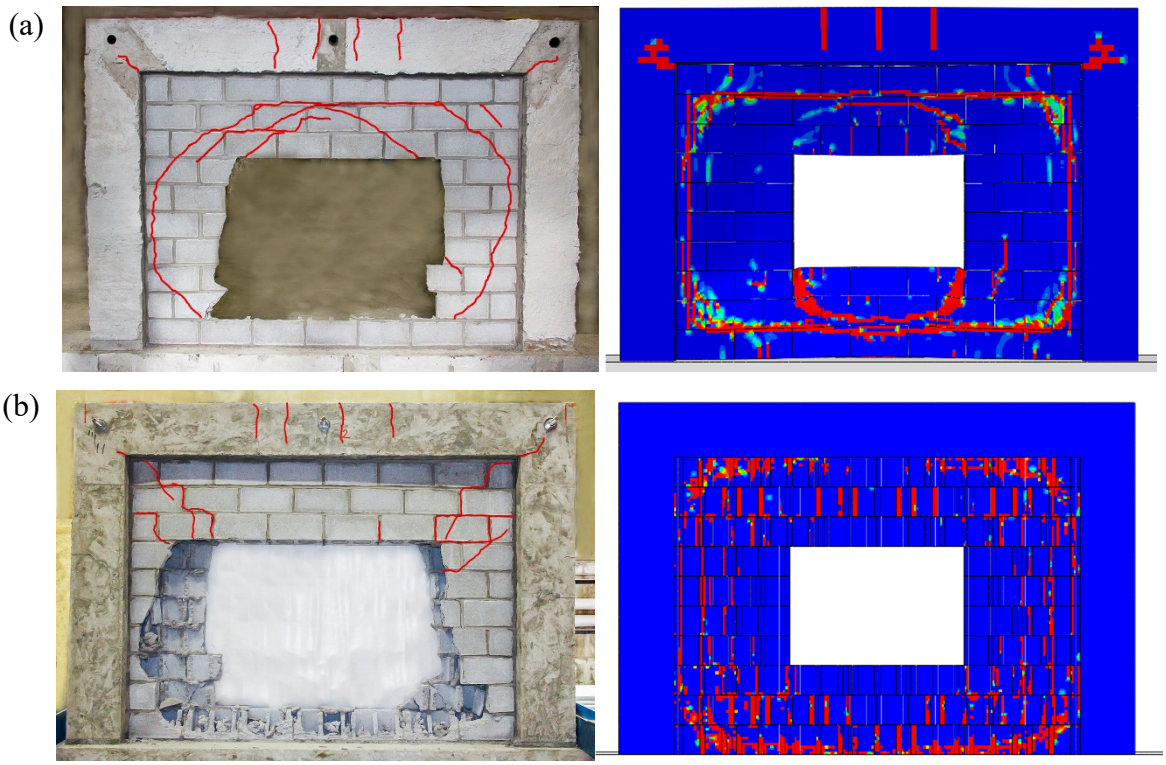

Figure 8: Comparison of FE and experimental results: (a) tensile cracks on the windward face and; (b) compressive crushing contours in the mid-plane of the infill

Figure 9 shows the progression of cracks on the web and faceshell of one of the CMUs from initiation of cracking till collapse of the wall. It is seen that cracking was first developed in the webs of CMUs. At ultimate, the webs showed pronounced shear failure which eventually caused instability of faceshells.

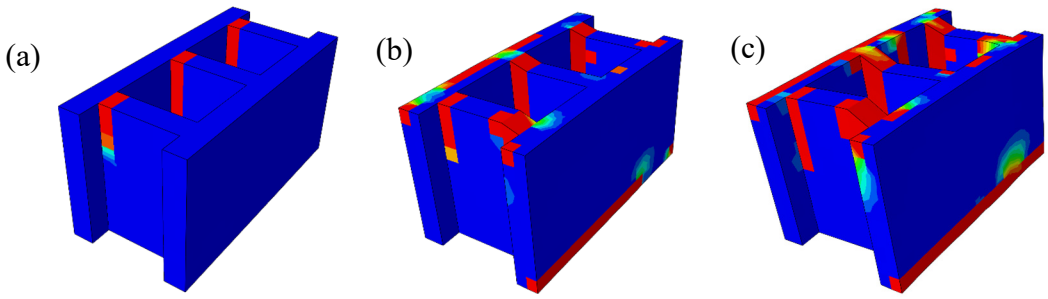

Figure 9: Development of cracks in the CMU blocks: (a) initiation of cracking; (b) at the ultimate capacity of the infill; and (c) after the collapse of the infill

CONCLUSIONS

A three-dimensional finite element model was developed to simulate behaviour of concrete masonry infilled RC frames subjected to out-of-plane loading. Details of model development for each component of infilled frame are described in the paper. An experimental program was on-going where the out-of-plane behaviour of infilled RC frame specimens was investigated. The results obtained so far for a regular as well as a specimen with infill opening were used in validation of the model. The results showed that the 3D model developed is capable of producing accurate ultimate strength results and simulating reasonably well the load vs. displacement behaviour. The cracking and failure modes of masonry infills were also captured by the FE model. Both experimental and FE results showed that cracking developed from the CMU webs initiated the failure of the infills. While further validation will be carried out when more results become available, the results so far show promise that the 3D modeling can provide detailed stress distribution, and simulate crack pattern and failure modes. A future study will include an investigation of effects of a wide range of material and geometric parameters on the out-of-plane behaviour of masonry infilled RC frames.

ACKNOWLEDGEMENTS

The authors wish to recognize the contribution of financial assistance by the Canadian Concrete Masonry Producers Association and Natural Sciences and Engineering Research Council of Canada.

REFERENCES

[1] Thomas F. The strength of brickwork. The Structural Engineer. 1953;31:35-46.
[2] McDowell E, McKee K, Sevin E. Arching action theory of masonry walls. J Struct Div. 1956;82:915.
[3] Gabrielsen B, Wilton C, Kaplan K. Response of arching walls and debris from interior walls caused by blast loading. DTIC Document; 1975.
[4] Gabrielsen B, Wilton C. Shock tunnel tests of arched wall panels. DTIC Document; 1974.
[5] Gabrielsen BL, Kaplan K. Arching in masonry walls subjected to out-of-plane forces1976.
[6] Dawe J, Seah C. Behaviour of masonry infilled steel frames. Canadian Journal of Civil Engineering. 1989;16:865-76.

[7] Maksoud A, Drysdale R. Rational moment magnification factor for slender unreinforced masonry walls. Proceedings of the 6th American Masonry Conf., Philadelphia, Pa1993. p. 6-9.
[8] Flanagan RD. Behavior of structural clay tile infilled frames. Oak Ridge National Lab., TN (United States); 1994.
[9] Angel R, Abrams DP, Shapiro D, Uzarski J, Webster M. Behavior of reinforced concrete frames with masonry infills. University of Illinois Engineering Experiment Station. College of Engineering. University of Illinois at Urbana-Champaign.; 1994.
[10] Flanagan RD, Bennett RM. Arching of masonry infilled frames: Comparison of analytical methods. Practice Periodical on Structural Design and Construction. 1999;4:105-10.
[11] Griffith M, Vaculik J. Out-of-plane flexural strength of unreinforced clay brick masonry walls. TMS Journal. 2007;25:53-68.
[12] Klingner R, Rubiano N, Bashandy T, Sweeney S. Evaluation and analytical verification of shaking ifw data from infilled frames. Part 2: Out-of-plane behavior. Proceedings of 7th North American Masonry Conference1996. p. 521-32.
[13] Thamboo J, Dhanasekar M. Nonlinear finite element modelling of high bond thin-layer mortared concrete masonry. International Journal of Masonry Research and Innovation. 2016;1:5-26.
[14] Noor-E-Khuda S, Dhanasekar M, Thambiratnam DP. Out-of-plane deformation and failure of masonry walls with various forms of reinforcement. Composite Structures. 2016;140:262-77.
[15] Minaie E, Moon FL, Hamid AA. Nonlinear finite element modeling of reinforced masonry shear walls for bidirectional loading response. Finite Elements in Analysis and Design. 2014;84:44-53.
[16] Bruggi M, Milani G, Taliercio A. Simple topology optimization strategy for the FRP reinforcement of masonry walls in two-way bending. Computers & Structures. 2014;138:86-101.
[17] Lourenco PB. Computational strategies for masonry structures: TU Delft, Delft University of Technology; 1996.
[18] Mehrabi AB, Shing PB. Finite element modeling of masonry-infilled RC frames. Journal of structural engineering. 1997;123:604-13.
[19] Lubliner J, Oliver J, Oller S, Onate E. A plastic-damage model for concrete. International Journal of solids and structures. 1989;25:299-326.
[20] Sima JF, Roca P, Molins C. Cyclic constitutive model for concrete. Engineering structures. 2008;30:695-706.
[21] Maekawa K, Okamura H, Pimanmas A. Non-linear mechanics of reinforced concrete: CRC Press; 2003.
[22] du Béton FI. Model code 2010: International Federation for Structural Concrete; 2012.
[23] Rots J. Numerical simulation of cracking in structural masonry. Heron. 1991;36:49-63.
[24] Atkinson R, Amadei B, Saeb S, Sture S. Response of masonry bed joints in direct shear. Journal of Structural Engineering. 1989;115:2276-96.
[25] Van der Pluijm R. Shear behaviour of bed joints. 6th North American Masonry Conference. Philadelphia, Pennsylvania, USA: Technomic Publ. Co; 1993.
[26] Masia MJ, Simundic G, Page AW. Assessment of the AS3700 relationship between shear bond strength and flexural tensile bond strength in unreinforced masonry. 2012.
[27] Lotfi HR, Shing PB. Interface model applied to fracture of masonry structures. Journal of structural engineering. 1994;120:63-80.
[28] CAN/CSA-A23.3-14 - Design of Concrete Structures. Canadian Standard Association; 2014.